SSSU 131
ISSN 0140 3818

Numerical Simulations of Mini 6.50 Composite Masts

Matteo Scarponi, Stephen Turnock, Ajit Shenoi

Ship Science Report No 131

October 2004

SSSU 131
ISSN 0140 3818

University
of Southampton

School of Engineering Sciences

Ship Science

Numerical Simulations of Mini 6.50 Composite Masts

Matteo Scarponi, Stephen Turnock, Ajit Shenoi

Ship Science Report No 131

October 2004

Numerical Simulations of Mini 6.50 Composite Masts

Matteo Scarponi, Stephen Turnock, Ajit Shenoi

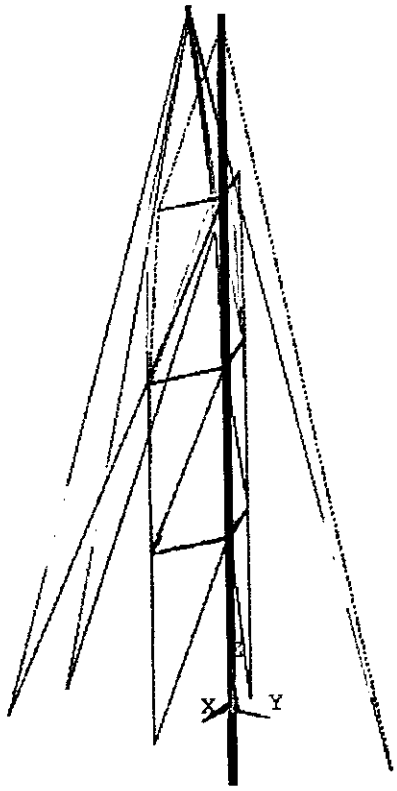

Ship Science Report No. 131
October 2004

School of Engineering Sciences
University of Southampton

Table of Contents

Chapter 1

Introduction

1.1 General principles

Performance and safety of a sailing yacht depend to a great extent on its mast and rigging design. The aim is to build a mast as light and aerodynamically efficient as possible, and to reduce the distance between the centre of gravity of the mast itself and the deck of the yacht. Masts are loaded by a combination of axial compressive forces and bending moments, therefore the risk of global buckling has to be considered when dimensioning cross sections and rigging layout. [3,4]

Therefore, it is easy to realize that mast design is a field where several issues need to be be taken into account: longitudinal and lateral stability, structure reliability, correct response to dynamic loading, low windage, ease of trim, lightness, costs. Over the years, such a complex design task has been accomplished in different ways, ranging from traditional rules of thumb for solid wooden masts to complex simulations where fluid-structure interaction issues are considered. Semi-empirical formulae have been adopted to estimate and assess mast compressions and loads acting on the standing rigging; today this method still serves most of the classification societies as a basis for their calculations. When the aim is the maximization of the performances of a racing sailboat, conventional design techniques become inadequate: the large safety factors commonly adopted for cruising yachts should be left aside and

the modeling of fluid-structure interaction phenomena should instead be carried out, in order to predict the mutual interaction between sails and rig. Complex numerical models are needed in order to predict the behaviour of composite materials adopted for mast tube and rigging and to estimate sail loads at different points of sail. Generally speaking, simulations allow designers to test wide ranges of design candidates and to select the most promising ones.

1.2 Project aims and objectives

The aims and objectives for the project are:

- Develop a FEM-based tool to predict mast shape under given external loads; analyses will be focused on mast prebend under given standing rigging loads
- Validate FEM results
- Apply the above tool to Mini-Transat class composite masts, in order to evaluate different rigging configurations (e.g. 2 vs 3 spreaders).
- Evaluate the possibility of carrying out DOE-based simulations by using the FEM-based tool.

1.3 Outline of the report

The present report consists of five chapters that can be summarised as follows:

- Detailed definition of the objectives of the project and different solutions for accomplishing them will be shown in the next Chapter. Then, choices for materials, mast design, standing rigging solutions and a relevant parameter set are accounted for.

- The guidelines for mast modeling, meshing and simulation are described in Chapter Three. The development of an ANSYS parametric macro for mast modeling and simulation will be analysed.
- The results of several set of simulations on different Mini Transat mast solutions and/or rigging tuning options will be accounted for in Chapter Four, focusing on 2 or 3 spreaders design options.
- Conclusions and future work are the subjects of Chapter Five.

Chapter 2

Mast design

2.1 Introduction

In the first stage of the present project, the FEM analysis of a mast model has to be set-up. The reference sailing class for the whole project will be the Mini 6.50: the choice of this class and its main features will be accounted for in the next paragraph.

The overall aim is to work out a fast and functional simulative strategy, accurate enough to be sensitive to small changes in the CAD model geometry (e.g. spreaders length, sweepback angle, panels span) and in loading conditions (e.g. shrouds, forestay tensions).

The issues of the present stage are:

- choice of a FEM software
- definition of a set of geometric and structural parameters, suitable for the most common mast solutions
- choice of an efficient modeling strategy (level of detail vs CPU time, parametric geometry)
- set-up of an automatic modeling and simulation procedure (through a macro and/or a programming language)

The FEM tool will be used to evaluate mast prebend under standing rigging preloads.

2.2 Mast/mainsail coupling, mast prebend

The mainsail is the sail that in any inventory has to cope with the widest range of wind speeds and angles. It must be capable of being "stretched" into almost every possible shape, through both tension and mast bend to cope with a wide wind range (direction and intensity). Along with offering considerable forward power to the boat, the sail also greatly affects the boat ability to track in a straight line. In short a mainsail set up will be the biggest effect on the balance of the boat much the same as a flap on an aircraft wing [10]. When a mast is tuned, the rigger aims at matching the mast trailing edge curve with a given mainsail luff: so, the main can keep its design shape (no kinks, no wrinkles, even draft distribution along sail span) and it becomes more sensitive to shape controls (such as runners, mainsheet, traveler, kicker, cunningham etc.), allowing the crew to *shift gears* easily, for instance to gain more power or pointing ability.

At the same time, considering long-distance offshore racers as Minis, enough tension should be given to standing rigging, in order to prevent mast breakdown in rough seas and strong breezes.

2.3 Mini 6.50 class

The Mini 6.50 m is an *open class*, which means that class rules define a *box* for the design, allowing a wide range of innovation, but ensuring equity of design for racing. The class rules focus on safety and the stability rules provide major design constraints.

The yacht has to be a mono hull, not exceeding 6.5 m length and 3 m beam, with a maximum draft of 2 metres. The top of the mast is at most 14 m

in distance from the underside of the keel. The maximum diameter of the bulb is 0.450 m and materials with higher density than lead are forbidden anywhere in the yacht.

The boat must comply with the following large and small angle stability requirements in order to ensure safe ballast system design [Class Rules, 2003].

- *Small angles stability:* the boat must not exceed a 10° heel angle in the most unfavourable ballast, mobile keel and mast configuration.
- *Large angles stability:* the boat must have positive stability with a 45 kg weight (not including the Archimedes effect) at the top of mast, in the most unfavourable conditions.

Further constructional constraints for the hull state that the cockpit must be 15 cm above waterline, a watertight bulkhead has to be situated between 5% and 15% of LWL and the freeboard has to be above 75 cm on average over the length of the boat.

The sail area is restricted by the boom length, which cannot extend beyond the transom with the main hoisted. No more than 8 sails can be carried including storm sails.

Conventional standing aluminium rigs with one or two spreaders were employed until Yves Parlier used a carbon mast in 1985, halving the mast weight. Some wingmast configurations were also used: according to Class Rules, a spar with a streamlined section is considered as a sail and therefore reduces to seven the number of sails that can be carried onboard while racing. Composite spars were banned in 1995, as to keep racing campaign costs down and to improve safety of Mini yachts. The latest version of the rule (2004) allows the use of carbon fibre composites for mast and rigging. There is no weight or chord length restriction for the mast, but its design cannot be altered

during the racing season and any replacement mast must be identical to the initial design.

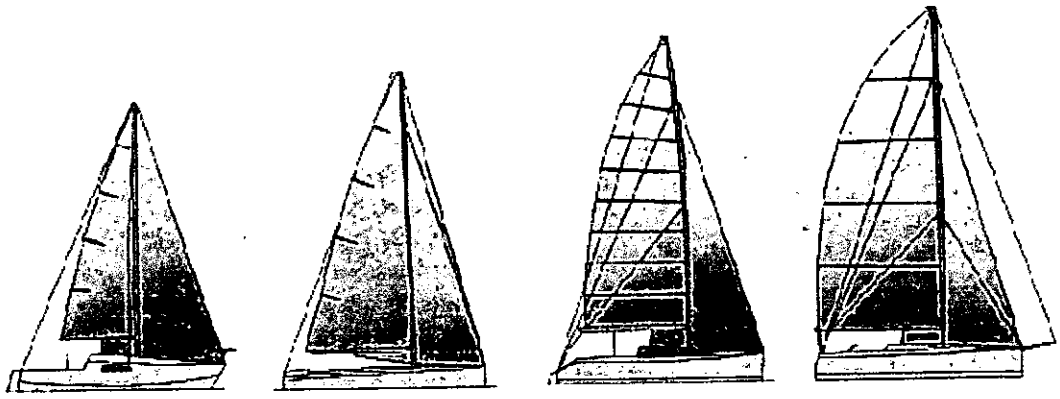

Fig. 2.1 – Mini 6.50 design evolution

2.4 Mast design and rigging layout

2.4.1 General design choices

After the most recent changes in the class rules (2004), composite masts and rigging are now allowed and the minimum weight limit has been removed: large improvements to aluminium masts can therefore be made and a large reduction in the weight of standing rigging may occur. This is why carbon masts and composite rigging only will be taken into account here.
Moreover, fractional rigs only will be considered: this is the solution adopted by the whole Mini fleet and it allows crews to use a fractional non-overlapping jib, a masthead spinnaker for light winds and a fractional spinnaker in strong winds. As far as the choice between deck-stepped or keel-stepped configuration is concerned, the latter option was chosen in [6] and the relative calculations are available; a keel-stepped configuration will be examined here

as well, but the mast model developed for FEA simulations was designed in order to switch easily to a deck-stepped layout.

Most of the design solutions of this project were already adopted in previous Mini designs carried out at Southampton University; for further information readers are referred to [6] and to its bibliography, where design choices are fully accounted for.

2.4.2 Mast tube

A tapered spar was designed in [6]; in the following table, the required transverse and longitudinal 2nd moments of area (mm^4) are shown for both spreaders options.

	3 spreaders		2 spreaders	
Panel #1	Ixx = 365521	Iyy = 1459920	Ixx = 625062	Iyy = 1459920
Panel #2	Ixx = 355779	Iyy = 1250785	Ixx = 566966	Iyy = 1121197
Panel #3	Ixx = 244977	Iyy = 1024956	Ixx = 258511	Iyy = 908827
Panel #4	Ixx = 140636	Iyy = 878976		

Table 2.1

Mast sections are developed through a trial and error process, in order to achieve the previously calculated moments of area; sections with a circular leading edge and a flat back were selected in [6]. In the present work, elliptical sections and tapered mast models are considered. At first, simulations relative to non-tapered spars were also carried out and validated: in that case, the moments of area to be achieved by the section were those of the 1st panel in each spreaders configuration (for extra safety).

	3 spreaders		2 spreaders	
mid-section size	122 x 51		120 x 66	
section thickness	0.287mm x 12 layers = 3.444mm		0.287mm x 12 layers = 3.444mm	
Panel #1	Ixx = 365521	Iyy = 1459920	Ixx = 625062	Iyy = 1459920

achieved quantities	Ixx = 381906	Iyy = 1474842	Ixx = 641259	Iyy = 1594858

Table 2.2

Each of the above curves was extruded along its normal in order to generate the mid-mast tube surface. If other mast shapes were needed, a possible approach could be to design the tapered part of the mast in a CAD environment, to import it into the selected FEA software and then to connecte it to the rest of the spar. In the present work, the tapered mast will be obtained by offsetting the selected tube section (taper ratio is calculated in order to achieve Table 2.1 quantities) and then by *skinning* such frame as described in Chapter 3.

The required section thickness is achieved while meshing the mast tube: shell elements for composite modeling, characterized by a user-defined number of layers, can be used for this purpose.

A commercial mast section (Stabmast "D"), developed for carbon spars with a built-in mainsail track, was also modeled and a 2 meters tube was tested through FEA, mainly to evaluate the CPU time required to carry out such analyses.

2.4.3 Spreaders

Generally speaking, spreaders are needed to diminish the free length of the mast tube and, as a consequence, to reduce the moment of inertia of the mast section: the required moment of inertia for the mast to carry a certain load is actually proportional to the free length squared.
Spreaders number and orientation is a key choice in Mini mast design: the top boats of the Mini fleet have 2 or 3 spreader rigs, so both solutions will be evaluated in this work. A three spreaders rig has reduced panels lengths and

sections with smaller second moments of area compared with a two spreaders rig. Some drawbacks are:

- increased probability of failure due to the increased number of rigging components;
- possibly higher windage.

Several 2 and 3 spreader rigs are available: some of them show a *jumper arrangement* where the jumper struts are normally angled forward. The purpose is to stay the top mast, not only athwartships, but also fore and aft [7]. The use of jumper struts enables the top mast to be given a more slender taper. Such an arrangement might be necessary when using a masthead spinnaker and/or for stabilising the top of the mainsail.

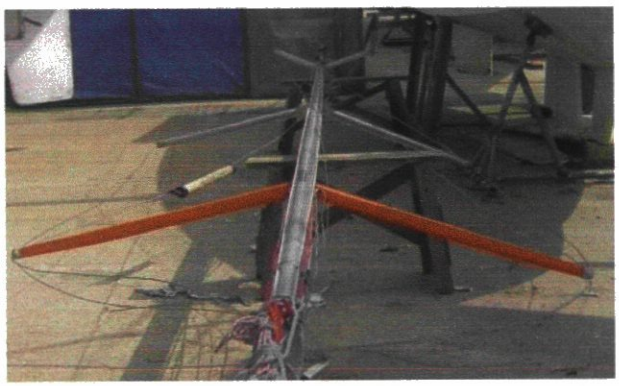

fig. 2.2 – two swept spreaders plus jumpers

2.4.4 Standing rigging

As suggested in [7], and according to the most recent Mini 6.50 rigging solutions, the following layout will be adopted:

- cap & diagonal shrouds
- forestay
- running stays (runners)
- one set of checkstays

As far as rigging materials are concerned, NAVTEC Nitronic 50 rod [8] was selected, according to what suggested by Allspars [9].
In the following pictures (Mini Fastnet 2004), four different Mini rigs can be seen:

Fig. 2.3.a - two inline spreaders

Fig. 2.3.b - two spreaders, conventional layout

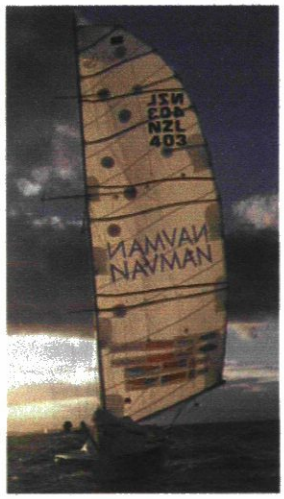

Fig. 2.3.c – three spreaders plus jumpers

Fig. 2.3.d - three spreaders, conventional layout

Conventional two and three spreaders layouts as in figures 2.3.b and 2.3.d were selected, modeled and simulated: the first of them (aluminium version & conventional rod rigging) is adopted in the most recent Mini production design: the well known *Pogo2*, designed by Groupe Finot.

Chapter 3

Set-up of mast structural simulations

3.1 Choice of a FEA software

FEM simulations of a mast subject to standing rigging loads can be carried out by means softwares where the following features are available:

- *built-in CAD modeling basic functions:* simple mast and rigging layouts should be modeled into the FEA environment; moreover, the user should be allowed to export such model in a common CAD interchange format;
- *reliable importation features* when a third-party CAD software has to be used for mast modeling (e.g. streamlined section for wingmasts);
- *finite elements* suitable for wires and ropes modeling; such elements should be capable of resisting tensile stress only, slack condition, pretensioning and large displacements should be supported;
- *composite materials shell elements* have to be available and complex composite lay-ups should be modeled, since carbon masts simulations are required;
- *batch programming language available*, so that simulations could be launched and results collected automatically; this is a fundamental requirement when large sets of simulation have to be carried out.

ANSYS software (by ANSYS, Inc.) was chosen for the task, since it fulfils all of the above requirements.

3.2 Mast modeling and meshing strategy

At first a fractional, keel-stepped, multiple spreaders mast model was set up, according to dimensions suggested in [6], where the rig was designed through conventional formulae. The standing rigging is composed of cap and intermediate shrouds, forestay, runners and checkstays; because of high camber mainsails, masthead runners are adopted instead of a backstay.

According to calculations carried out in Ch.2, two elliptical, zero-thickness sections were modeled in a third-party CAD software (Rhinoceros) and then used in ANSYS environment, in order to test ANSYS import features and to evaluate the most efficient interchange format; sections in IGES format (filename.igs) were correctly imported in the FEA environment with the following options:

No defeaturing	yes	Create solid if applicable (SOLID)	no
Merge coincident keypoints (MERGE)	yes	Delete small areas (SMALL)	no

The possibility of modeling the whole tube outside ANSYS was evaluated. Unfortunately, the tube couldn't be imported as a single entity, but just as a patchwork of surfaces; furthermore, duplication of lower geometry entities (points and lines) occurred, making it necessary to delete them before starting to mesh. In the present approach, non-tapered mast tubes are modeled by extruding a given elliptical section, in order to allow a mapped meshing through quadrilateral shell elements. Each mast panel is obtained through its own extrusion operation, so that immediate spreaders generation is allowed. Tapered masts are obtained in a different way: 1st panel section is offset of a given ratio, so that design moments of inertia can be achieved for all panels, then such frame undergoes skinning in order to generate the tube. Obviously, the latter approach could also suit the modeling of a non-tapered mast, but it

leads to a less rational numbering of geometric entities created this way (keypoints, lines and areas), so extrusion of section was selected when applicable. Neither spreaders nor rigging are modeled at this stage: those entities will be generated while meshing, so just spreader tips, rigging chainplates and shrouds and stays attachment points to mast are generated as ANSYS *keypoints*.

With an available mast tube model, meshing operations can be performed and the whole rigging can be generated as follows: shell elements (SHELL99) are adopted for the composite spar, beam elements (BEAM4) for spreaders, while link elements (LINK10) are used for standing rigging. This elements choice leads to a very effective FEA model, when low CPU time is required to carry out simulations; this is particularly desirable when sets of simulations must be carried out on a conventional PC with the purpose of showing the trends of a phenomenon (eg. consequences of an increase in sweepback angles). Further details about the chosen finite elements will be given in the next paragraph, where the whole ANSYS macro will be analyzed.

3.3 ANSYS macro

Unlike interactive mode, ANSYS batch programming mode allows the user to work through macros (.mac files): a set of FEM simulations can be easily launched and results can automatically be collected and saved. The written macro shows the following features:

- choice of finite elements
- definition of a set of real constants
- definition of material properties
- definition of mast parameters

- rig modeling
- meshing
- postprocessing (e.g. plot of deformed shape and structure displacements, exportation of deformed nodes coordinates)

3.3.1 Choice of finite elements

SHELL99 element was selected to model the composite spar. It may be used for layered applications of a structural shell model and it allows up to 250 layers to be modeled; if more than 250 layers are required, a user-input constitutive matrix is available. Fibers orientation can also be controlled by the user. The element has 6 DOF at each node: translations in the nodal x, y and z directions and rotations about the nodal x, y and z axes. The element is defined by eight nodes, average or corner layer thicknesses, *layer material direction angles* (fibers orientation) and orthotropic material properties. Midside nodes may not be removed from this element.

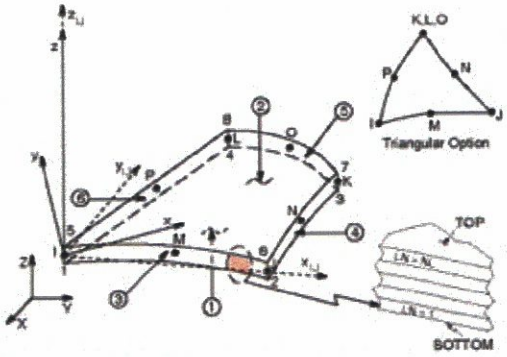

LN = Layer Number

NL = Total Number of Layers

Fig. 3.1 - SHELL99

BEAM4 elements are used to model spreaders. They are uniaxial elements with tension, compression, torsion, and bending capabilities. The element has six degrees of freedom at each node: translations in the nodal x, y, and z directions and rotations about the nodal x, y, and z axes. Stress stiffening and

large deflection capabilities are included. The element is defined by two or three nodes, the cross-sectional area, two area moments of inertia (IZZ and IYY), two thicknesses (TKY and TKZ), an angle of orientation (θ) about the element x-axis, the torsional moment of inertia (IXX), and the material properties.

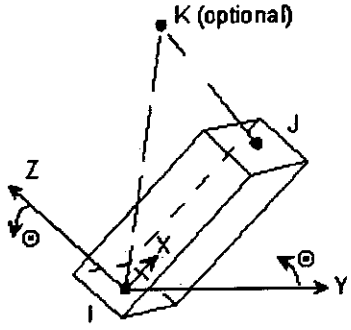

if node K is omitted and Θ = 0°, the element y axis is parallel to the global X-Y plane

Fig. 3.2 - BEAM4

LINK10 (tension-only or compression-only spar) is used for standing rigging. It is a three-dimensional spar element with the feature of a bilinear stiffness matrix resulting in a uniaxial tension-only (or compression-only) element. With the tension-only option, the stiffness is removed if the element goes into compression (simulating a slack cable condition). According to ANSYS documentation, this feature suits static guy wire applications where the entire guy wire is modeled with one element. LINK10 has three degrees of freedom at each node: translations in the nodal x, y, and z directions; moreover, large deflections capabilities are available. Different real constant sets have been implemented for each part of the standing rigging; real constants for LINK10 include *cross-sectional area* of cable and *initial strain*. Wire pretension can be introduced by assigning a value to the *initial strain* (ISTRN) variable.

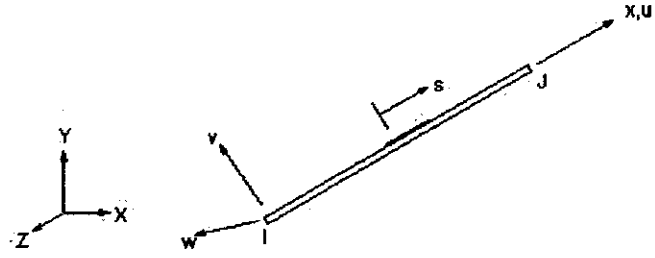

if node K is omitted and Θ = 0°, the element y axis
is parallel to the global X-Y plane

Fig. 3.3 - LINK10

3.3.2 Definition of real constants sets and material properties

The following set of material properties was adopted and associated with SHELL99 element:

MP,EX,1,165E9	elastic moduli
MP,EY,1,50E9	
MP,EZ,1,50E9	
MP,NUXY,1,.28	minor Poisson's ratios
MP,NUYZ,1,.28	
MP,NUXZ,1,.28	
MP,GXY,1,50E9	shear moduli
MP,GYZ,1,50E9	
MP,GXZ,1,50E9	

As for spreaders section, a hollow NACA 16-021 "Ring Wing" profile was selected in [6]; the following second moment of inertia (I) and section modulus (SM) values were obtained through *Larsson & Eliasson* formulae:

		I (mm^4)	SM (mm^3)
3 spreaders	Lower	14559	3399
	Middle	13163	1660
	Upper	7660	624
2 Spreaders	Lower	13163	2140
	Upper	7660	787

Table 3.1 - Required 2nd moment of area and section modulus for spreaders

while in Table 2.5 sections data that meet the above design requirements are shown:

		Chord (mm)	No.of plies	thickness(mm)	I (mm^4)	SM (mm^3)
3 spreaders	Lower	90	7	2	15302	3511
	Middle	90	6	1.7	13641	3077
	Upper	75	7	2	8382	2037
2 spreaders	Lower	90	6	1.7	13641	3077
	Upper	75	7	2	8382	2037

Table 3.2 - Spreaders sections data

Since an optimization of spreaders design goes well beyond the purposes of this analysis, spreaders are considered here just as rods capable of transmitting standing rigging loads to a mast tube without undergoing relevant deformations. For extra simplicity, steel mechanical properties were supplied to BEAM4 MP set, whose syntax is as follows:

```
MPDATA,EX,2, ,210E9
MPDATA,PRXY,2, ,0.28
```

A set of real constants for BEAM4 can be supplied as follows:

```
R,set_number,AREA,Izz,Iyy,Tkz,Tky
```

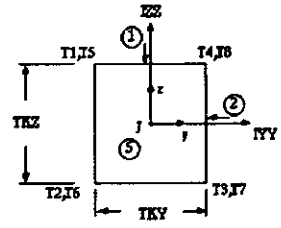

Fig. 3.4 - BEAM4 section

It can be easily shown that data in Table 3.1 are matched through a 90mm x 12.5mm rectangular section, which fulfils both the three spreaders and the two spreaders design requirements. The following R set is then provided:

```
R,2,0.00012,14559E-12,759375E-12,0.0125,0.09
```

As far as standing rigging is concerned, the following options are available according to [6]:

1 *Dyform Wire*: lower stretch and greater strength compared with other wire types of a similar diameter;
2 *Composite Rod*: aramid fibres are pultruded into a rod which is approximately 25% lighter than rods and wires with the equivalent stretch and has a higher breaking strength;
3 *Nitronic Rod*: it is generally 20% stronger and has 40% less stretch than wire of the same diameter. Although slightly heavier than wire, rod will stretch 10% less than wire of the same weight.

A comparison between mechanical properties of the above materials can be found in Table 3.3 [8]:

rigging type	diameter (mm)	min. breaking load (kg)	stretch (mm/m/1000kg)	weight (g/m)
1*19 Dyform wire	5	2440	3.737	135
Aramid Rod	5.6	2931	3.212	32
N50 Rod	4.37	2140	3.389	118

Table 3.3

N50 Nitronic Rod by Navtec Rigging Solutions Ltd was selected in [6]: such a solution will be also adopted here as a starting point for mast simulations. Standing rigging material properties are taken into account in the ANSYS macro through real constant sets with the following syntax:

```
R,Real_Constant_Set_Number,AREA,ISTRN
```

where AREA stands for cable cross-sectional area and ISTRN refers to cable initial strain. For simplicity's sake, cable diameter is kept constant to 4.37 mm for the whole standing rigging.

Several real constant sets were set up, so that each standing rigging element has its own set; this feature allows each cable to be tuned (through its own ISTRN value) independently from the others. The *Excel* spreadsheet *rigging_preloads.xls* was written in order to calculate ISTRN values on a set of rigging wires under given cable tensions.

```
! shrouds: Vi (i = 1,2) & D3
R,3,1.5E-5,0.000678,

! shrouds: D1 & D2
R,4,1.5E-5,0.000678,

! forestay (if ISTRN < 0 = slack)
R,5,1.5E-5,-0.000339,

! running stays (if ISTRN < 0 = slack)
R,7,1.5E-5,-0.000339,

! checkstays (if ISTRN < 0 = slack)
R,8,1.5E-5,-0.000170,
```

3.3.3 Choice of a set of parameters

In order to perform a static analysis of a Mini 6.50 mast subject to rigging loads, the following quantities were parametrized:

- number, length and sweepback angle of spreaders
- span of each mast panel
- mast tube taper ratio
- initial rake angle (*THETA*) of the unloaded mast
- tension of each cable element (through the *initial strain* value)
- height of checkstays attachment points to the mast
- position of shrouds and stays chainplates on deck

The above parameters are assigned a value at the beginning of the ANSYS macro; .mac files can therefore be read more clearly and changes in the rigging layout are made easier.

3.4 Tapered mast modeling

In order to obtain a closer modeling of the actual mast geometry, a tapered spar was designed. The elliptical shaped sections referred to in the above paragraphs are still adopted: such sections will be just scaled over the mast span to achieve the required Ixx and Iyy values shown in Table 3.4. The design choice is to keep a constant section thickness and fibers lay-up all over the spar; anyway ANSYS gives the user the opportunity to drop one or more layers, so a variable thickness mast can be implemented as well.
Given the geometry of the lower panel section, scale factors for the other mid-panel sections were calculated as to achieve the aforementioned Ixx and Iyy values. Sections were then positioned and shifted aft, as to obtain a straight mast trailing edge (mainsail groove or batten-cars traveler). Unlike the constant section mast case, no extrusions can obviously take place here, therefore sections were *skinned* (ASKIN function) to generate the mast surface. This technique obviously leads to small geometrical discontinuities where mast panels join, but the errors are considered largely negligible.

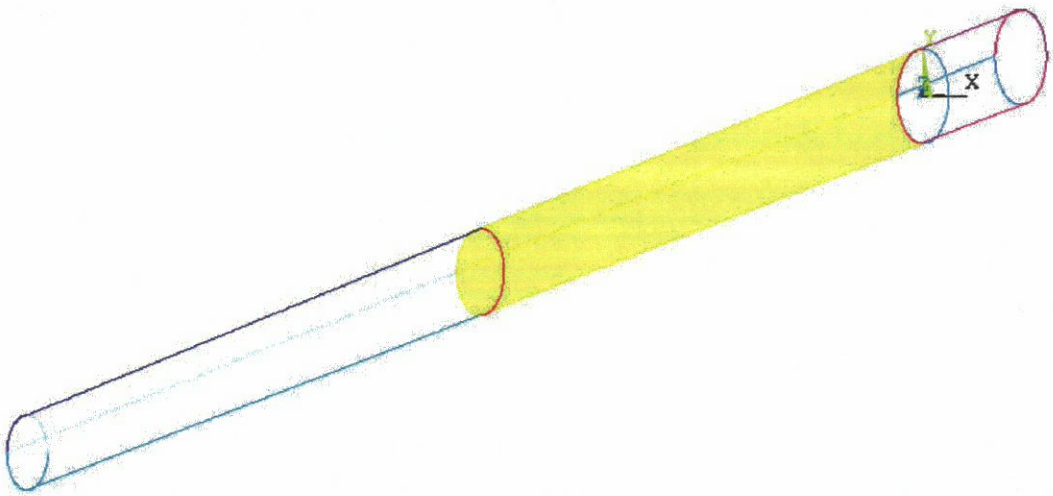

Fig 3.5 - mast generation by skinning existing sections

Additional sections need to be created at this stage: some are needed for meshing purposes while other ones are necessary to place keypoints over the mast. The following keypoints are generated:

- standing rigging attachment (eg. D3 for a two spreaders rig);
- forestay, runners and checkstay attachments;
- spreaders roots.

Sections are generated through boolean splitting (area by area, *ASBA* function): the final mast topology for two spreaders case is shown below.

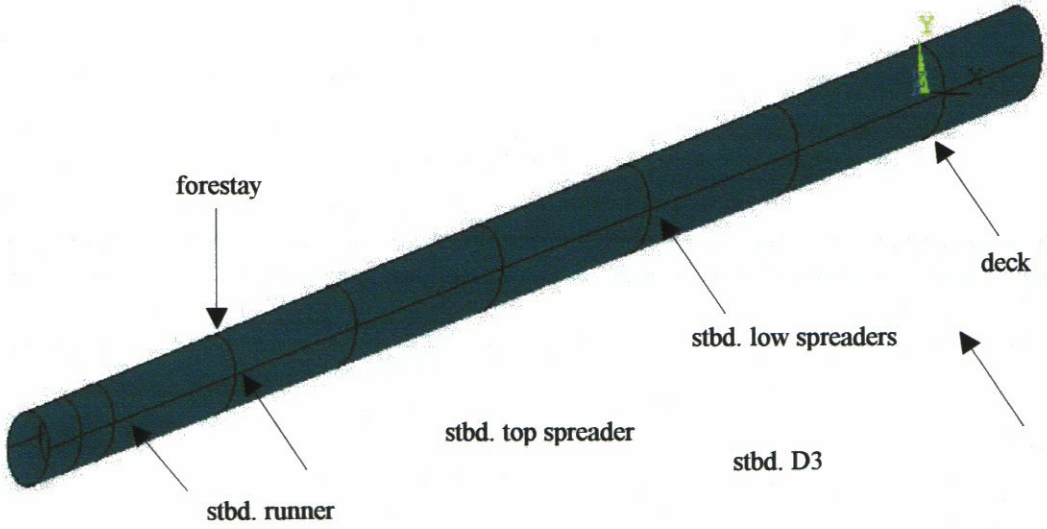

Fig. 3.6 - two spreaders mast configuration

3.5 Meshing

Model meshing strategy follows the overall project guidelines: to minimize CPU time in order to carry out quickly a set of parametric simulations; therefore, when meshing the mast tube, a quadrilateral mapped mesh was preferred to non-structured options. Several mast meshing strategies were attempted: at first simulations with uniform grids were carried out, with ESIZE values ranging from .02 to .08. Results, expressed in terms of maximum nodal displacement (which occurred at masthead), were then compared with the outcome of a variable sized grid. The latter shows small elements at deck level, close to spreader roots (Fig. 3.8) and to forestay attachment; above all, it requires a different modeling technique. As a matter of fact, a single panel can be meshed by quadrilateral elements of variable size through the LESIZE function: the user can choose, for instance, the number of divisions NDIV along an area border and the spacing ratio SPACE. If SPACE parameter is positive, nominal ratio of last division size to first division size (if > 1.0 sizes increase, if < 1.0 sizes decrease). If negative, |SPACE| is nominal ratio of center division(s) size to end divisions size. Ratio defaults to 1.0 (uniform spacing).

Unfortunately, a single line can't be meshed with a double-sided spacing ratio option, so a single mast panel can't show a fine mesh at the ends and a coarse mesh at mid-span. Anyway, the needed refinement can be obtained by halving each panel through a boolean splitting (area by area, *ASBA* function), so that each half can be meshed separately from the other.

Default spacing ratio adopted was 2.5; it is supplied to the ANSYS macro as the additional FL_RATIO parameter.

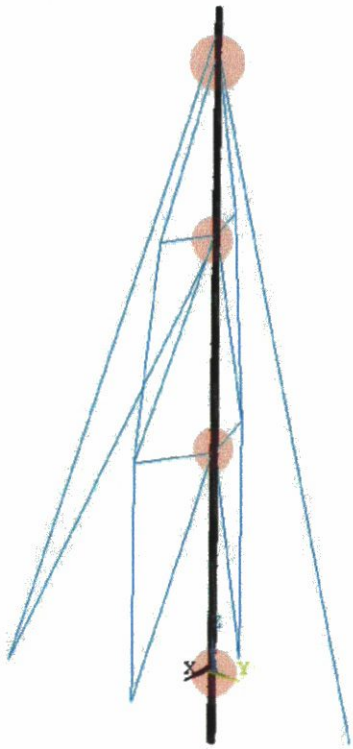

fig. 3.7 - mesh refinement (shaded areas)

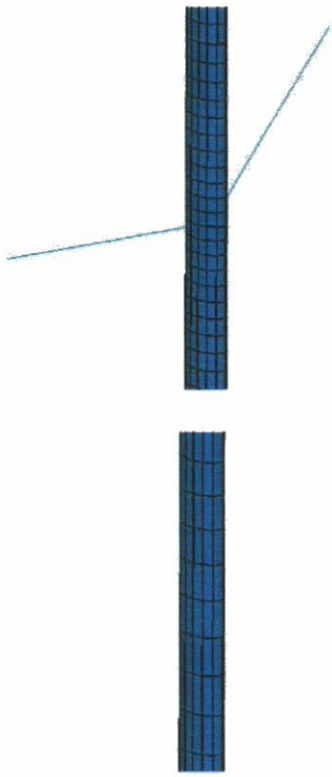

fig. 3.8 – min and max mesh size

The following table summarizes a set of simulations carried out on the same 2-spreader mast subject to constant loads and different meshing options. Displacements of masthead node on trailing edge are shown: since no relevant differences between results can be appreciated, a compromise between CPU time and grid refinement can be achieved with the variable sized option (4th row)

ESIZE	UX	UY	UZ	USUM
.02	0.12482E-04	0.22574E-01	0.81570E-05	0.22574E-01
.04	0.37130E-05	0.22289E-01	0.75958E-05	0.22289E-01
.08	0.17692E-05	0.22937E-01	0.75266E-05	0.22937E-01
variable	**0.46606E-05**	**0.22293E-01**	**0.62153E-05**	**0.22293E-01**

Table 3.4

Spreaders were meshed in order to allow the whole model to undergo buckling analysis: such meshing wouldn't make sense if such a test wasn't performed,

since spreaders are considered here just as beam elements capable of transferring shrouds load to the mast.
According to ANSYS meshing guide, every rigging cable was modeled through a single LINK10 element.

3.6 Postprocessing

After each structural simulation, the shape of mast trailing edge needs to be evaluated and plotted: a MATLAB piece of code was set up for this purpose. The postprocessing steps are the following:

1) At the end of the simulation, all lines belonging to the undeformed mast trailing edge are selected and their nodes are sorted in ascending Z order. Nodes coordinates are then exported and written to a text file (nodes_list.txt)
2) Nodal displacements are then taken into account and the Ux, Uy, Uz fields are appended to the output text file (nodes_list.txt).
3) Two .m files were written in order to plot results:

ANSYS_translator.m (subroutine) reads data from text file and fills up two n-by-3 matrices: *nodes* and *displ*, then ***mast_plot.m*** (main program) gets those data and plots three graphs out of them. In the first one, initial and deformed groove shapes are compared, while in the other two, camber and %camber amount over mast span are plot. Moreover, the position and amount of maximum camber are displayed.
The above three graphs summarize simulation results as far as final mast shape is concerned: this shape can then be compared with a given mainsail luff curve. MATLAB code for postprocessing purposes can be found in *Appendix A*.

Chapter 4

Simulations results and postprocessing

4.1 Purposes of simulations

Several sets of simulations were carried out with the following purposes:

- to check the overall performances of the system (macro and postprocessing routines)
- to evaluate the influence of some of the selected parameters on mast deformed shape and to consider if other quantities should be parametrized
- to estimate the range of variation for each parameter (do mast inversions or S-shaped displacements occur?)

Not all model features are actually used: runners and checkstays were kept unloaded either in two and three spreaders simulations.

4.2 Two spreaders rig simulations

forestay	cap shr.	diag. shr.	runners	checkstays	theta
100kg	300kg	150kg	slack	slack	0.0

Table 4.1

At first, tensions on cap shrouds, diagonal shrouds and forestay were kept constant and spreaders sweepback angle was changed over the range 15° to 35° (same angle for both spreaders). As Figures 4.1 and 4.3 show, increasing sweepback angle without changing standing rigging tensions leads to higher amount of mast rake without significant changes in camber distribution. The modeled mast looks quite stiff, though the loaded forestay reduces prebend, since all simulations show quite a small amount of camber. Mast trailing edge curve is smooth, without knees due to tapering or spreaders insertion. The top panel doesn't undergo significant bending: this could be obtained through higher taper ratios (without compromising mast strength), thinner sections (composite layers can be dropped at 2/3 of mast span) or through higher sweepback angles for the top spreader.

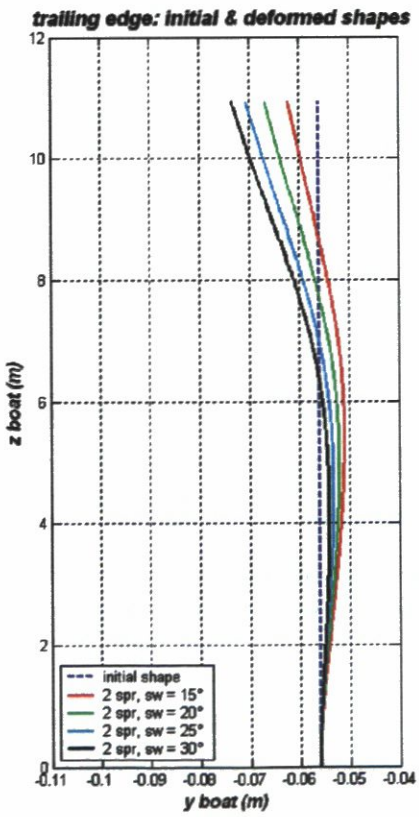

Fig. 4.1

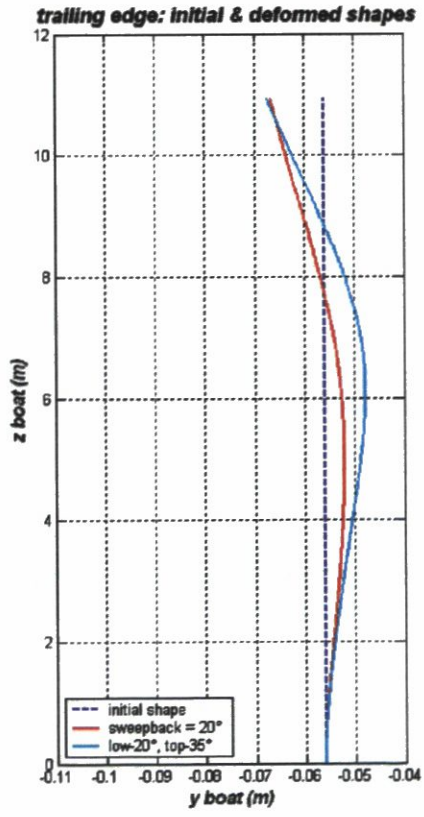

Fig. 4.2

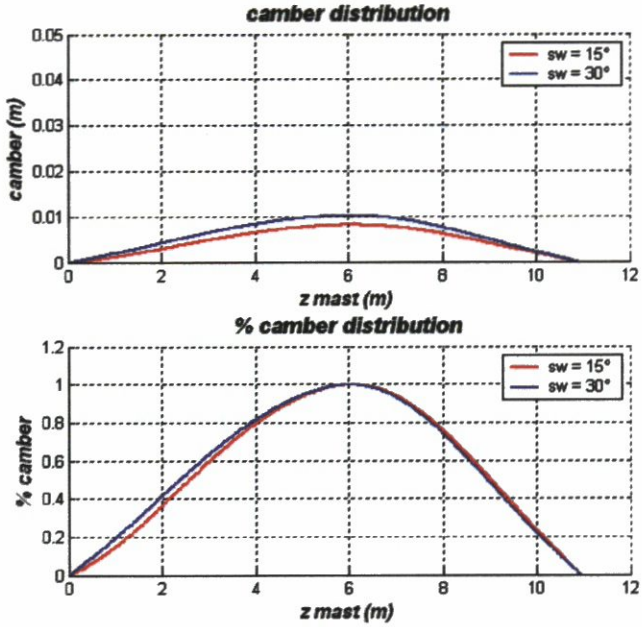

Fig. 4.3

Then, top spreader sweepback angle was modified (values = 25°, 30°, 35°) while keeping constants all tensions and other parameters; a 20° swept low spreaders are adopted in this set of simulations. Results are shown in Fig. 4.2: mast camber increased when top spreader sweepback angle increased to 35°, while no relevant differences in masthead displacement occurred.

Let us consider the influence of forestay load on mast prebend: because of its placement, any increase in forestay tension should pull forward the top of the mast and then diminish prebend. Three load conditions were simulated: mast prebend with a slack forestay is compared with displacement fields due to 50 kg and 100 kg load; shrouds tensions were set as in Table 4.1, while sweepback angles were kept costant (20° for both spreaders). Fig. 4.4 shows that results are consistent with the above remarks; in Fig. 4.5 a gradually

decreasing camber is shown, despite the shape of the top third of the mast isn't affected by the increased load.

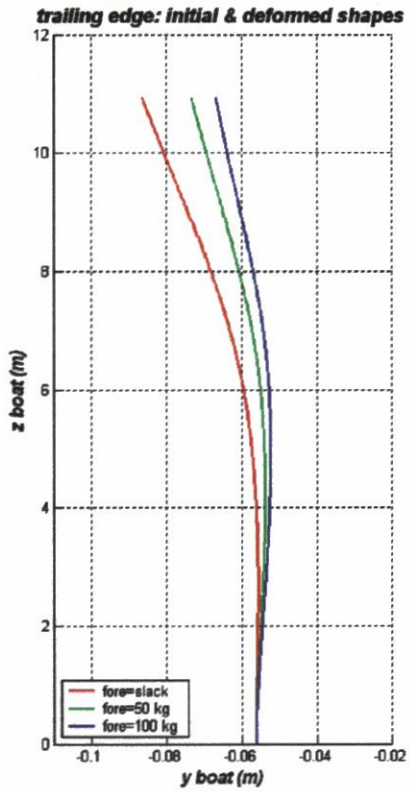

Fig. 4.4

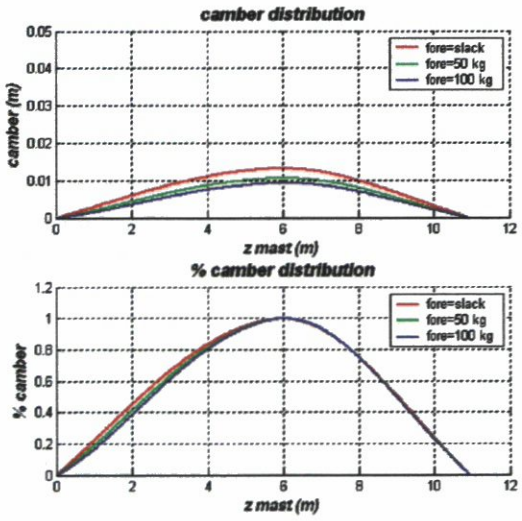

Fig. 4.5

Let us consider variations in the undeformed mast orientation: as suggested by several rigging/tuning guides (e.g. Hallspars mast assembly manual), considerable gains in prebend can be achieved this way. Prebend is strictly related to the location of the mast step: most mast steps have fore-and-aft slots to facilitate adjustment. With a keel stepped mast fixed at the deck with wedging, a slight adjustment of mast step position affects prebend. There are other methods: generally the mast is chocked with wedges to position it to the designed (or rated) J, therefore a rearrangement in wedging invariably leads to a change in prebend. In the ANSYS model the unloaded mast rake can be changed supplying *theta* angles other than zero, where *theta* is the parameter that takes into account rotations about x-axis of the "mast" coordinate system with respect to "boat" coordinate system. The effects of wedges can also be simulated: a given y-displacement field (where y is the fore-aft direction) is given to mast collar section before to launch FEM simulation. The following graphs show results of 10, 20 and 30 mm displacement fields at mast collar height and orientated towards +y axis, which is to say that wedges are pushing the mast forward; the loaded shape without wedges is also shown, to allow a comparison.

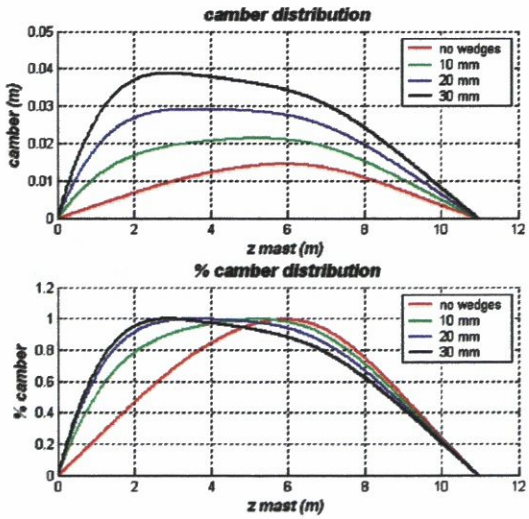

Fig. 4.7

Position of maximum camber moves towards deck as wedges thickness increase, and the overall depth of the lower third of the mast is greatly affected as well. Just two more observations: the top third of the mast looks pretty straight and reluctant to bending: the loaded shape develops a knee at top spreaders level that never occurs when the mast is wedge-free.

4.3 Three spreaders rig simulations

Forestay	cap shr.	diag. shr.	runners	checkstays	theta
100kg	200kg	50-150kg	slack	slack	0.0

Table 4.2

As in the previous set of simulations, tensions on cap shrouds, diagonal shrouds and forestay were initially kept constant and spreaders sweepback angle was changed over the range 15° to 35° (same angle for all of the spreaders). Just like two spreaders case, any increase in sweepback angle without changing standing rigging tensions leads to higher mast rake values without significant changes in camber distribution. In the present example, a slight inversion can be noticed over the first panel at the higher sweepback angles, while no concavity change occurs below 30°.

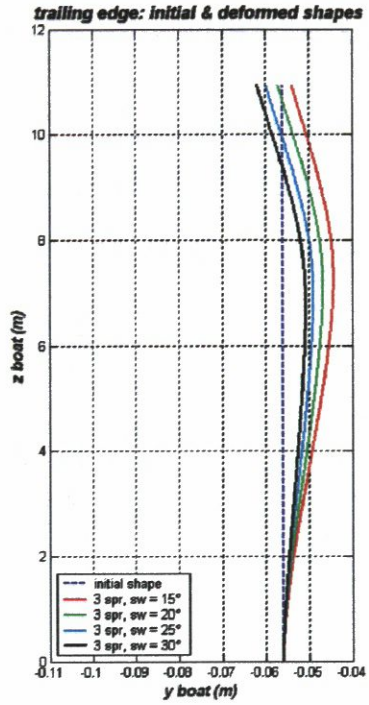

Fig. 4.5

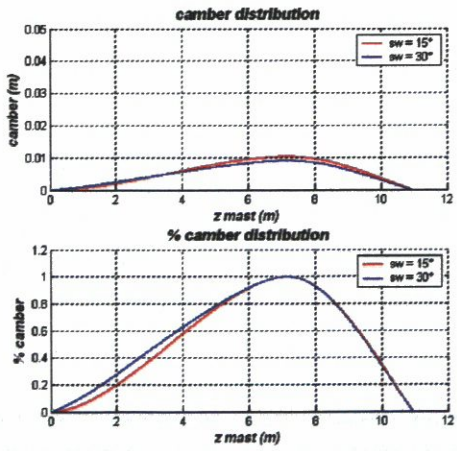

Fig. 4.6

Other simulations were carried out in order to estimate the effect of variations in diagonal shrouds (D1, D2, D3) tensions while keeping all other parameters constant. Both 20° and 30° swept spreaders cases were taken into account,

with diagonal shrouds loads varying in the range 50 to 150 Kg. Results for 50, 75 and 100 kg for both sweepback angles are shown below.

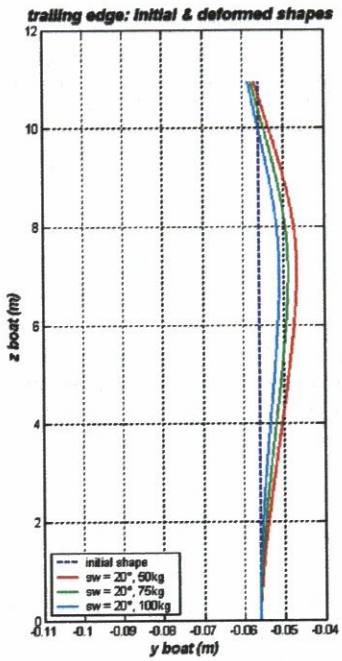

Fig. 4.7

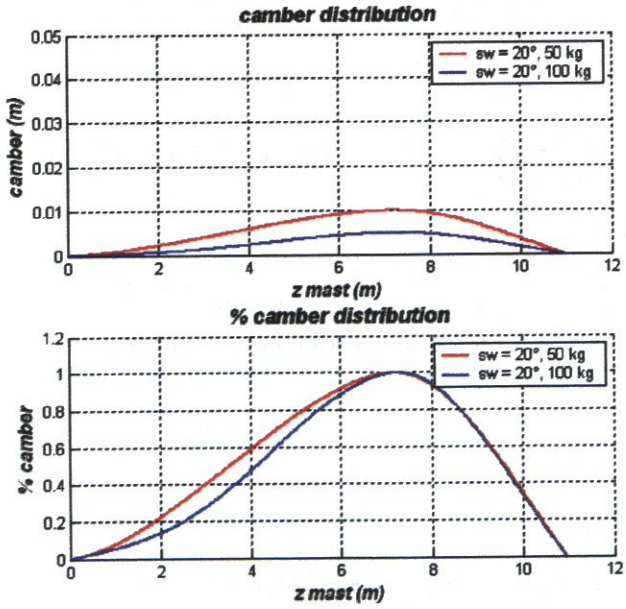

Fig. 4.8

As for 20° swept spreaders, the model develops increasing amounts of prebend with decreasing tensions on D1, D2 and D3s: camber amount with a 50kg load is nearly two times the camber at 100 kg. Masthead node basically keeps its undeformed position; maximum camber height (z coordinate) is also constant. In the graphs shown below, results relative to 30° swept spreaders are represented. Camber trend with increasing loads is the same as in 20° case and %camber graphs are nearly coincident at 50 and 100 kg, but the overall deformed shapes look different.

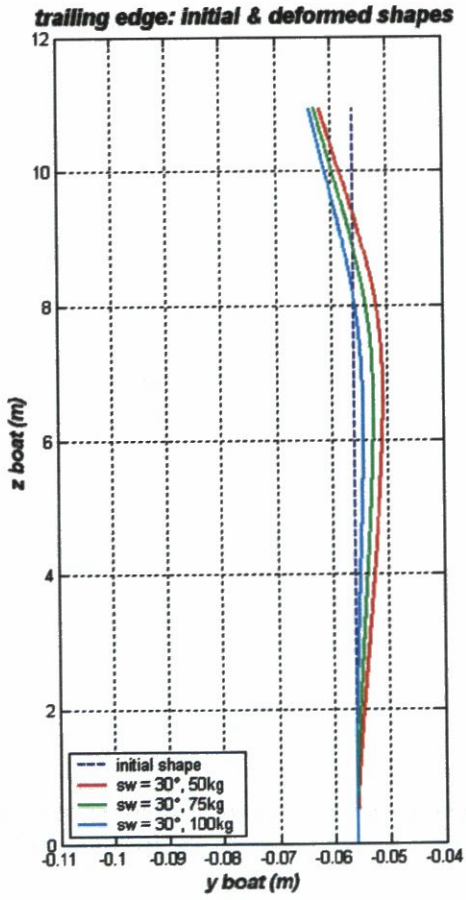

Fig. 4.9

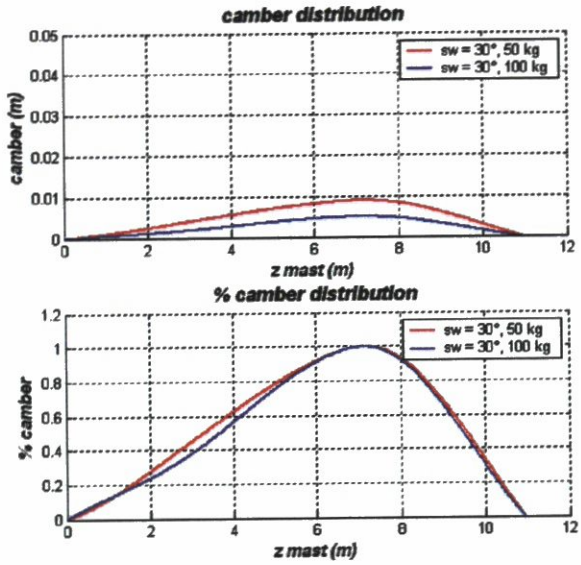

Fig. 4.10

With diagonal shrouds loads over 100 kg, mast inversion occurs: this is particularly evident with 20° swept spreaders (when lower aft-bending forces due to shrouds develop). Higher vertical loads are stressing mast tube, which is unsupported by runners and checkstays, so that buckling deformations occur.

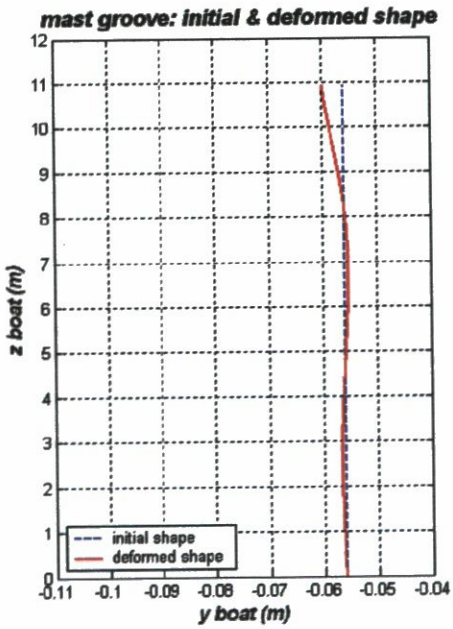

Fig. 4.11

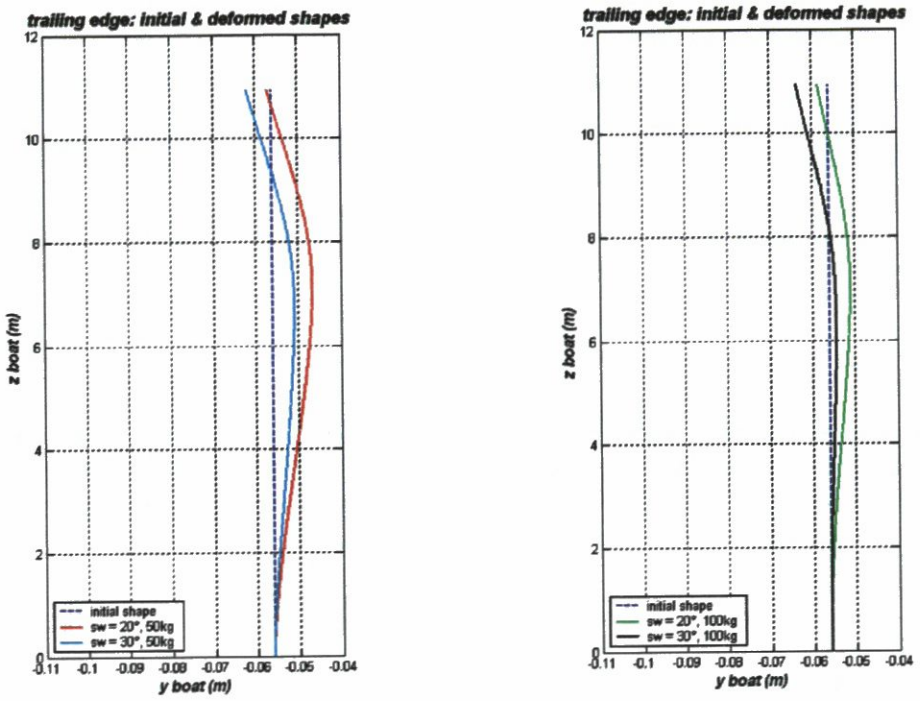

Fig. 4.12

In Fig. 4.12, deformations at different sweepback angles and same tensions on D_i (i = 1 to 3) are compared: when spreaders angles are small, aft bending forces due to shrouds' tensions decrease, so that the mast is pulled further forward by forestay load.

Chapter 5

Conclusions and future work

5.1 Conclusions

In this report, a method to simulate the behaviour of composite masts was worked out. Several sets of FEA simulations were carried out on MINI 6.50 mast models with two and three spreaders layouts, rigged and tuned in several ways, in order to show how geometrical and structural parameters affected mast prebend. ANSYS batch programming language allowed to work through entirely parametric macros and to store simulations results in text files; postprocessing was carried out through MATLAB pieces of code, for immediate visualization of results.

Parametric analyses on keel stepped, composite, tapered Mini masts were carried out and nearly all quantities affecting prebend were taken into account: shrouds and stays tensions, mast taper ratio, number and sweepback angle of spreaders, wedging, position of mast foot.

The designed mast models allowed to carry out sets of parametric simulations in a short time (less than 1 minute on a conventional Pentium IV laptop): lots of effort was spent in finding the best compromise between an effective modeling and a reduction in CPU time. The use of composite shell elements for mast tube and mapped meshing are the most relevant features on this side.

The method for FEA tests coupled with postprocessing routines proved to be suitable for a DOE-based set of simulations: all of the selected parameters had a relevant influence on mast prebend, even if attention has to be paid to their range of variation (e.g. settings leading to mast inversions have to be discarded).

A validation of the above results was worked out for elementary loading condition, both for aluminium and composite spars: displacements predicted through FEA were matched.

5.2 Future work

A detailed modeling of a commercial composite Mini 6.50 mast should be carried out, paying attention to the actual material/s and lay-up used, mast tube sections and rigging solutions. For validation purposes, shrouds and stays tensions and the resulting displacement fields should be measured, allowing the user to get some feedback on numerical results and therefore to correct the model, where necessary.

DOE-based simulations should then be carried out, in order to give the user as many information as possible about trends shown by a given rig with the minimum number of simulations.

The next and most challenging step is obviously to add sail loads to the model: FEA of the mast could be integrated in an iterative fluid-structure interaction routine, where aerodynamic loads on sails (and mast) could be evaluated at each step by a CFD model and sails displacements as a response to the above loads could be calculated in a separate FEA model. A routine to evaluate the net field of pressure over asymmetrical spinnakers and the relative sailcloth displacements is available at Dipartimento Ingegneria

Industriale, Università degli Studi di Perugia (Italy) and could be a reliable starting point for such work.

Appendix A

MATLAB files for postprocessing

A.1 Example of ANSYS output text file

```
SORT ON ITEM=LOC    COMPONENT=Z      ORDER= 1   KABS= 0   NMAX=     7372
SORT COMPLETED FOR      365 VALUES.

LIST ALL SELECTED NODES.    DSYS=   0
SORT TABLE ON  Z
```

NODE	X	Y	Z	THXY	THYZ	THZX
498	0.0000	-0.60000E-01	0.0000	0.00	0.00	0.00
1418	0.0000	-0.60031E-01	0.17694E-01	0.00	0.00	0.00
1419	0.0000	-0.60062E-01	0.35388E-01	0.00	0.00	0.00
1420	0.0000	-0.60094E-01	0.53631E-01	0.00	0.00	0.00
1421	0.0000	-0.60125E-01	0.71873E-01	0.00	0.00	0.00
1422	0.0000	-0.60158E-01	0.90682E-01	0.00	0.00	0.00
1423	0.0000	-0.60191E-01	0.10949	0.00	0.00	0.00

```
(snip)
```

nodal displacements are appended to the above list as follows (displacements in X direction only are shown)

```
PRINT U     NODAL SOLUTION PER NODE
***** POST1 NODAL DEGREE OF FREEDOM LISTING *****

LOAD STEP=      1   SUBSTEP=      1
TIME=     1.0000       LOAD CASE=    0

THE FOLLOWING DEGREE OF FREEDOM RESULTS ARE IN GLOBAL COORDINATES

    NODE       UX
     498    0.0000
    1418 -0.44821E-08
```

```
    1419 -0.84892E-08
    1420 -0.13408E-07
    1421 -0.18809E-07
    1422 -0.24636E-07
    1423 -0.30934E-07

(snip)
```

A.2 ANSYS_translator.m

```
path_nodes='C:\ANSYS_work\nodes_list.txt';
fid_nod=fopen(path_nodes,'r');

nodes = [];
displ = [];
X_disp = [];
Y_disp = [];
Z_disp = [];
while ~feof(fid_nod)
  line = fgetl(fid_nod);
  switch line
        case {'    NODE      UX    '};
          flag = 'X';
        case {'    NODE      UY    '};
          flag = 'Y';
        case {'    NODE      UZ    '};
          flag = 'Z';
        otherwise
  end
  a = str2num(line);
  if ~isempty(a) & size(a)==[1 7]
    nodes = cat(1,nodes,a);
  elseif ~isempty(a) & size(a)==[1 2] % allora e' una coppia nodo & spostamento
nodale
     switch flag
         case {'X'}
           X_disp = cat(1,X_disp,a(1,2));
         case {'Y'}
           Y_disp = cat(1,Y_disp,a(1,2));
         case {'Z'}
           Z_disp = cat(1,Z_disp,a(1,2));
         otherwise
     end
  end
end
```

```
status = fclose('all');
displ = [X_disp Y_disp Z_disp];
```

A.3 mast_plot.m

```
ANSYS_translator

Units = 'pixels';
scr = get(0,'ScreenSize');

[a,b] = size(nodes);      % a = numero di nodi considerati
def_nodes = zeros(a,3);  % def_nodes contiene le coord nodi deformata
cam_index = 0;
for j = 1:3
 def_nodes(:,j) = nodes(:,j+1)+displ(:,j);
end

nnodes = sortrows(nodes,4);          % sort nodes, ascending Z coord (mast axis
direction)
ddef_nodes = sortrows(def_nodes,3); % sort ddef_nodes, ascending Z coord (mast axis
direction)

figure('Position',[30, 350, 400, 550])
plot(nnodes(:,3),nnodes(:,4),'b--','Linewidth',2);
grid on
hold on
plot(ddef_nodes(:,2),ddef_nodes(:,3),'r-','Linewidth',2);
title('\it\bf{mast groove: initial & deformed shape}','FontSize',14)
xlabel('\it\bf{y boat (m)}','FontSize',12)
ylabel('\it\bf{z boat (m)}','FontSize',12)
legend('initial shape','deformed shape',3)
axis ([-0.1 0.1 0 12]);
set(gca,'XTick',-0.09:0.005:-0.05)
set(gca,'XTickLabel',{'-0.090','','-0.080','','-0.07','','-0.06','','-0.05'})
set(gca,'YTick',0:1:12)
set(gca,'YTickLabel',{'0','1','2','3','4','5','6','7','8','9','10','11','12'})

m = (ddef_nodes(a,3)-ddef_nodes(1,3))/(ddef_nodes(a,2)-ddef_nodes(1,2));
q = ddef_nodes(a,3) - m*ddef_nodes(a,2);
freccia = zeros(a,1);
for i = 1:a
 freccia(i,1) = abs(ddef_nodes(i,3)-m*ddef_nodes(i,2)-q)/((1+m^2)^0.5);
 if freccia(i,1) >= max(freccia)
     cam_index = i;
 end
```

```
end

camber = max(freccia);
position_vect = [def_nodes(cam_index,2)-def_nodes(1,2) def_nodes(cam_index,3)-
def_nodes(1,3)]; %approssimata
position = norm(position_vect);
chordlength_vect = [def_nodes(a,2)-def_nodes(1,2), def_nodes(a,3)-def_nodes(1,3)];
chordlength = norm(chordlength_vect);

figure('Position',[440, 350, 600, 550])
subplot(2,1,1);
plot(ddef_nodes(:,3),freccia(:,1),'Linewidth',2);
title('\it\bf{camber distribution}','FontSize',14);
xlabel('\it\bf{z mast (m)}','FontSize',12);
ylabel('\it\bf{camber (m)}','FontSize',12);
axis([0 11 -0.01 0.03]);
grid on

stri_camb = ['\it\bf camber = ', num2str(round(camber*1000)), ' mm'];
stri_posi = ['\it\bf position = ', num2str(round(position*1000)), ' mm'];
text(5,0,stri_camb,...
     'HorizontalAlignment','right',...
     'EdgeColor','red',...
     'BackgroundColor',[1 1 1],'FontSize',14);
text(5,-0.005,stri_posi,...
     'HorizontalAlignment','right',...
     'EdgeColor','red',...
     'BackgroundColor',[1 1 1],'FontSize',14);

subplot(2,1,2);
plot(ddef_nodes(:,3),freccia(:,1)/max(freccia),'Linewidth',2);
title('\it\bf{% camber distribution}','FontSize',14);
xlabel('\it\bf{z mast (m)}','FontSize',12);
ylabel('\it\bf{% camber}','FontSize',12);
axis([0 11 -0.02 1.02]);
grid on

posi = ['\it\bf position = ', num2str(round((position/chordlength)*100)), '%'];
text(5,0.1,posi,...
     'HorizontalAlignment','right',...
     'EdgeColor','red',...
     'BackgroundColor',[1 1 1],'FontSize',14);
```

Appendix 2

Bibliography

[1] Larsson L, Eliasson R, *Principles of Yacht Design*, McGraw-Hill, UK 2001

[2] Claughton A, Wellicome J F, Shenoi R A, *Sailing Yacht Design, Theory*, Longman, UK 1998

[3] Nijhof A H J, *Carbon Fibre Reinforced Spars and Masts*, Delft University of Technology

[4] Enlund H, Pramila A, Johansson P G, *Calculated and Measured Stress Resultants in the Mast and Rigging of a Baltic 39 Type Yacht*, Int. Conf. On Design considerations for Small Craft. London, 1984

[5] Boote D, *Mast and Rigging Design*, Sailing Yacht Design: Theory, Longman, UK 1998

[6] Giocosa A, Schulze-Hagenest T, Shaw S, Vanneste A, Verrier M, *Design of a Mini-Transat 6.50*, University of Southampton - Meng group design project, 2004

[7] *Hints and advice on rigging and tuning Seldén masts*, 2004

[8] NAVTEC Rigging Solutions Ltd, http://www.navtec.net/home/index.cfm

[9] Allspars website, http://www.allspars.co.uk/minitransat.html, http://www.xs4all.nl/~blvrd/html/carbonmasts.html

[10] North Sails online technical articles, http://www.northsails.co.uk/media/articles/mainsail.html